Dehydration promotes intracellular lipid synthesis and accumulation

Joshua S. Carty[1], Jazlyn Selvasingh1, Yvonne Zuchowski[1], Hyuck-Jin Nam[2], Clothilde Pénalva[2], Gayani Nanayakkara[2], Erin Q. Jennings[3], Kelsey Voss[4], Edith T. Adame[1], John T. Tossberg[1], Wei Sheng Yap [5,6], Meiling Melzer[1], Olga Viquez[1], A. Scott McCall[7], Elizabeth R Piotrowski[8], Ryoichi Bessho[1], Shirong Cao[1], Katrina L. Leaptrot[9], Alexandra C. Schrimpe-Rutledge[9], Simona G. Codreanu[9], Stacy D. Sherrod[9], John A. McLean[9], Jonathan B. Trapani[1], Matthew A. Cottam[10], Ma Wan[11], Deepti Shrivastava[11], Don Delker[11], Matthew H. Wilson[1,12], Clinton M. Hasenour[13], Louise Lantier[13], Irene Chernova[14], Jamey D. Young[13,15], Volker H. Haase[1,12,13], Jose Pablo Vazquez-Medina[8], Dylan K. Kosma[16,17], Peter Kim[5,6], Jean-Philippe Cartailler[10],Mingzhi Zhang[1], Roy Zent[1,12], Raymond C. Harris[1,12], Jason A. Watts[11], Andrew S. Terker[1], Fabian Bock[1], Jeffrey C. Rathmell[18], Aylin R. Rodan[2,19,20] and Juan P. Arroyo*[1,13,21]

Abstract:

Lipids can be considered a water reservoir used to offset dehydration stress as their oxidation by the mitochondria generates water. However, whether dehydration directly regulates lipid synthesis is unknown, which is the focus of this study. We found that dehydration stress decreases cellular oxygen consumption, increases intracellular lipid synthesis, and favors glutamine oxidation as a carbon precursor for lipid synthesis via remodeling mitochondrial metabolism. These findings provide a mechanism whereby cellular dehydration leads to intracellular lipid accumulation, functionally linking water availability to lipid storage.

Affiliations:

[1] Division of Nephrology and Hypertension, Vanderbilt University Medical Center; 1161 21st Ave South, Nashville, TN, 37232, USA.
[2] Molecular Medicine Program, Spencer Fox Eccles School of Medicine, University of Utah; Salt Lake City, UT 84112
[3] Division of Hematology and Oncology, Department of Medicine, Vanderbilt University Medical Center; 1161 21st Ave South, Nashville, TN, 37232, USA.
[4] Department of Pathology Microbiology and Immunology, Vanderbilt University Medical Center; 1161 21st Ave South, Nashville, TN, 37232, USA.
[5] Cell Biology Program, Hospital for Sick Children, Peter Gilgan Centre for Research and Learning; Toronto, ON, Canada.
[6] Department of Biochemistry, University of Toronto; Toronto, ON, Canada.
[7] Division of Allergy, Pulmonary, and Critical Care, Department of Medicine, Vanderbilt University Medical Center; 1161 21st Ave South, Nashville, TN, 37232, USA.
[8] Department of Integrative Biology, University of California; Berkeley, CA, 94720, USA.
[9] Department of Chemistry and Center for Innovative Technology; Vanderbilt University, Nashville, TN, 37232
[10] The Vanderbilt Creative Data Solutions Shared Resource, Vanderbilt University; Nashville, TN, 37232
[11] Epigenetics and RNA Biology Laboratory, National Institute of Environmental Health Sciences, National Institutes of Health; Research Triangle Park, NC 27709, USA
[12] Research and Medical Services, Department of Veterans Affairs, Tennessee Valley Healthcare System; Nashville, TN, 37232 USA.
[13] Department of Molecular Physiology and Biophysics, Vanderbilt University; Nashville, TN, 37232 USA.
[14] Section of Nephrology, Department of Internal Medicine, Yale School of Medicine; New Haven, CT, USA.
[15] Department of Chemical and Biomolecular Engineering, Vanderbilt University; Nashville, TN, 37232 USA.
[16] Department of Biochemistry and Molecular Biology, University of Nevada, Reno, NV 89557, USA
[17] Hitchcock Center for Chemical Ecology, University of Nevada, Reno, NV 89557, USA
[18] Vanderbilt Center for Immunobiology, Department of Pathology, Microbiology, and Immunology, Vanderbilt University Medical Center; Nashville, TN, 37232 USA.
[19] Division of Nephrology & Hypertension, Department of Internal Medicine, Spencer Fox Eccles School of Medicine, University of Utah; Salt Lake City, UT 84112
[20] Medical Service, Veterans Affairs Salt Lake City Health Care System; Salt Lake City, Utah, 84148
[21] Department of Cell and Developmental Biology, Vanderbilt University; Nashville, TN, 37232 USA.

*Corresponding author. Email: juan.p.arroyo@vumc.org

Introduction

Water is necessary for life and dehydration stress is common to most life forms on earth. Consequently, organisms with lifelong limited access to free water have developed mechanisms to generate water from lipids. However, it is currently unknown whether there is a direct mechanism through which dehydration stress regulates lipid storage and breakdown.

Water that is generated within an organism is known as metabolic water. Marine mammals (e.g., *pinnipeds* and *cetaceans*) do not consume sea water, rather they rely on metabolic water production for the maintenance of water homeostasis (*1*). Similar observations on the reliance on metabolic water have been made in birds (*2*) and camels (*3*). Metabolic water is mainly generated as a byproduct of the oxidation of lipids, carbohydrates, and proteins in the mitochondria. Lipid oxidation is the most efficient precursor for metabolic water generation, as beta-oxidation yields about 100 g of water for every 100 g of palmitate that is oxidized. This is almost twice as much as the water produced by the oxidation of glucose or protein (*4*). Therefore, in the appropriate context, lipid accumulation represents water storage.

While much is known about lipid metabolism in the context of energy balance, the role of dehydration stress in lipid metabolism is unclear (*5-9*). In plants, exposure to hypertonic stress can trigger the accumulation and subsequent breakdown of lipids (*6, 7, 10-15*). When an organism is dehydrated, extracellular fluid tonicity increases, which promotes intracellular water efflux, and compromises cell survival. Therefore, the acute accumulation of lipids can provide cells a way to store water in a non-diffusible form that can later be accessed by the cell through lipid oxidation once extracellular and intracellular tonicity are matched. Thus, we hypothesized that increases in extracellular tonicity, i.e., dehydration stress, triggers intracellular lipid accumulation. In this study, we demonstrate that dehydration stress directly promotes intracellular lipid synthesis by remodeling mitochondrial metabolism.

Results

Hypertonic stress promotes intracellular lipid synthesis and accumulation

The kidney, particularly the medulla, experiences wide variations in extracellular tonicity (-0.5-to-4-fold relative to serum osmolality, i.e. 150 mOsm/Kg – 1200 mOsm/Kg in humans) under physiologic conditions. Thus, the kidney is an ideal organ to understand the physiologic impact of hypertonic stress on cellular lipid metabolism. To test whether hypertonic stress promotes lipid accumulation, we treated kidney collecting duct (CD) cells with 100 mmol NaCl in lipid-free medium (to eliminate the possibility of increased uptake) and measured intracellular lipid droplet abundance. We found a significant increase in both the number and size of the lipid droplets in the NaCl treated collecting duct cells (Fig. 1A).

The rate limiting step for lipid synthesis is the activation of acetyl-coA carboxylase (ACC). Both ACC1 and ACC2 isoforms, which convert acetyl-coA to malonyl-coA that is used to synthesize fatty acids (*16, 17*), are expressed in the kidney (*18, 19*). They can be inhibited by AMP-activated protein kinase (AMPK) through phosphorylation of a carboxy-terminal serine residue, S79 and S221 in ACC1 and 2, respectively. Activating phosphorylation of AMPK during energy depletion favors phosphorylation (pACC-S79/221) and inhibition of ACC function, reducing lipid synthesis (Fig. 1B). Hypertonic NaCl stress in kidney medullary collecting duct cells resulted in ACC dephosphorylation and activation (Fig. 1C). 200 mM mannitol also dephosphorylated ACC, indicating the response is to hypertonic stress (fig. S1A). Activating phosphorylation of AMPKa T172 (pAMPKα-T172) was

decreased by hypertonic stress (fig. S1B). Thus, hypertonic stress inhibits AMPK, activates ACC and favors intracellular lipid synthesis.

Next, we investigated if this response also occurred *in vivo*. Water restriction can increase murine kidney medullary interstitium tonicity to over 3500 mOsm/Kg (relative to the ~300 mOsm/Kg in blood) to favor water reabsorption from the tubules into the blood. As water is retained, urine is concentrated and urine osmolality (UOsm) increases. We water restricted or water loaded wild-type C57BL/6J mice. We found that UOsm and whole kidney lysate triglyceride levels were higher in water-restricted mice (Fig. 1D, E). Water-restricted mice also had less pACC-S79/S221, consistent with increased ACC activation and lipid synthesis (Fig. 1F). In the collecting ducts of the water-restricted mice (identified by the water channel aquaporin 2, AQP2 which is upregulated and apically localized during water restriction (*20*)), where the extracellular tonicity is highest, we saw near absent phosphorylation of pACC-S79/S221 (Fig. 1G) as well as increased intracellular lipid content (Fig. 1H). These results suggest hypertonic stress favors the intra-cellular accumulation of lipids both *in vitro* and *in vivo*.

To test whether this mechanism exists in animals that rely on metabolic water production, we used primary endothelial cells from elephant seal (*Morounga angustirostris*). When these cells were challenged with lipid-free NaCl stress we saw that pACC- S79/S221 decreased significantly, consistent with ACC activation (Fig. 1I). These results suggest that the effect of hypertonic stress on lipid accumulation can also occur in animals that rely on metabolic water.

To understand hypertonicity-induced lipid synthesis, we performed global untargeted lipidomic LC-MS/MS analysis to characterize the changes that occur after exposure to hypertonic stress in CD cells (fig. S2). We found a significant increase in overall length of all lipids analyzed (fig. S3A), and an increase in various lipid species with the most significant being ether-linked long-chain triacylglycerols and cardiolipins (Fig. 2A, fig. S2), the latter of which are critical to maintaining mitochondrial membrane integrity (*21, 22*). In parallel, RNA-sequencing showed an enrichment in lipid synthetic pathways and a decrease in oxidative phosphorylation pathways in CD cells exposed to hypertonic stress (fig. S3B). These data further suggest that hypertonic stress results in the upregulation of lipid synthesis *in vitro*.

To dissect the metabolic changes associated with hypertonic stress, we performed live cell metabolic profiling of CD cells. Salt-induced hypertonic stress resulted in decreased oxygen consumption rates (OCR) and decreased extracellular acidification (ECAR), indicating a shift toward a more quiescent energy profile (Figure 2B). To test whether there are accompanying changes in mitochondrial morphology, we analyzed the mitochondrial aspect ratio of collecting duct cells treated with NaCl vs. controls. Hypertonic stress induced an increase in mitochondrial aspect ratio consistent with mitochondrial elongation, an adaptive strategy to maintain membrane potential and ATP production during cell stress (Fig. 2C) (*23-25*). Hypertonic stress also caused mitochondrial elongation (fig. S4A) and decreased mitochondrial membrane potential (fig. S4B) in HeLa cells, in which decreased OCR with hypertonic stress was previously observed (*26*). Together, these data suggest that hypertonic stress decreases cellular metabolism and increases lipid synthesis.

Transcription factor NFAT5 is required for hypertonicity induced lipid accumulation

Nuclear factor of activated T-Cells 5 (NFAT5), also known as tonicity-responsive enhancer-binding protein (TonEBP), is a transcription factor that regulates the cellular response to hypertonic stress (*8*) and has been implicated in the regulation of fat mass (*27*). Total body knockout of *Nfat5* is embryonic

lethal (*28*), but a haploinsufficient mouse model lacking one copy of *Nfat5* is protected from obesity when fed a high-fat diet, suggesting NFAT5 plays a critical role in lipid metabolism (*27*). Hypertonicity increased ACC activity by decreasing S79/221 phosphorylation, while *Nfat5* knockdown decreased ACC activity, increased AMPK activity (fig. S1C), and decreased intracellular lipid synthesis and accumulation in NaCl-treated CD cells (Fig. 3 A,B fig. S1C). To test if NFAT5 activation was required *in vivo* to promote lipid accumulation in the kidney, we used a haploinsufficient *Nfat5* knockout model, *Nfat5*$^{tm1a(KOMP)Wtsi}$, herein referred to as *Nfat5* heterozygous KO (Fig. 3C) (*29*). Following water restriction NFAT5 heterozygous KO mice had lower kidney lysate triglyceride content compared to wild-type controls, despite similar UOsm (*30*) (Fig. 3C). Together, these data show that NFAT5 is a critical component of hypertonicity-induced lipid synthesis and accumulation in cells and *in vivo*.

Hypertonic stress-induced lipid synthesis requires glutamine oxidation

Lipid synthesis requires a carbon source. Glucose-derived pyruvate can be converted to acetyl-CoA via pyruvate dehydrogenase (PDH) and further metabolized by the tricarboxylic acid (TCA) cycle to citrate, a precursor for fatty acid synthesis (Fig. 4A). However, NaCl treatment of CD cells increased inhibitory phosphorylation of PDH serine 293, a site phosphorylated by pyruvate dehydrogenase kinase 1 (Fig. 4B), as also observed previously in HeLa cells exposed to hypertonic stress (*26*). We therefore examined glutamine (*31, 32*) as an alternative carbon precursor for lipid synthesis (Fig. 4A). Intracellular glutamine concentration increased in CD cells after treatment with NaCl (Fig. 4C). In cells exposed to hypertonic stress, removal of glutamine from the cell medium resulted in inhibitory ACC phosphorylation (Fig. 4D) and decreased intracellular lipid content (Fig. 4D, fig S5). Thus, glutamine is critical to the lipogenic response to hypertonicity.

To further understand the importance of glutamine for the *in vivo* response to hypertonicity, we examined *Drosophila melanogaster* mutants. *Drosophila* have a single *NFAT* gene that is most homologous to mammalian *NFAT5* (*33*). Flies with a large deletion in *Drosophila NFAT, NFAT*$^{\Delta ab}$ (*33*), had higher lethality than controls under water-restricted conditions, which was worsened by hypertonic stress from high salt feeding and further exacerbated by dietary glutamine restriction (Fig 4E, fig. S6). In contrast, wet starvation conditions (i.e., access to water but no food) had no effect on mortality in any group, confirming that mortality is driven by lack of water rather than lack of calories (fig. S6, S7). Conversely, dietary supplementation with an additional 25 mM glutamine for seven days prior to water restriction abolished the excess lethality seen with high salt exposure in both control and *NFAT* mutant flies (Fig. 4F), further highlighting the need for both glutamine and NFAT function in the response to hypertonic stress.

Glutamine can be converted to the lipid precursor, citrate, via oxidative or reductive TCA cycling (Fig 4G) (*31, 32*). We treated NaCl-exposed CD cells with uniformly labeled ^{13}C glutamine to understand the metabolic fate of glutamine under hypertonic stress. The abundance of carbon-13 (i.e., ^{13}C-enriched) isotopologues of citrate/isocitrate M+2, M+4, and M+6 were elevated after salt treatment relative to controls (Fig. 4H); moreover, reductive carboxylation of α-ketoglutarate to citrate (M+5) was minimal in both NaCl- and control-treated collecting duct cells (Fig. 4G, H). These results show that hypertonic stress promotes glutamine incorporation into the TCA cycle in the oxidative direction.

We then explored if hypertonic stress promotes glutamine incorporation into the TCA cycle *in vivo*. Glutamine carbons primarily enter the TCA cycle via glutaminase (GLS) conversion of glutamine to glutamate, and glutamate dehydrogenase (GDH) conversion of glutamate to α-ketoglutarate. *D.*

melanogaster mutants in which *Gls* or *Gdh* were knocked down in the renal epithelium (Malpighian tubule) had significantly higher mortality in response to NaCl hypertonic stress (Fig. 4I, fig. S8A), as did wild-type flies fed the GLS inhibitor, BPTES (fig. S8B). Wet starvation had no effect on mortality (fig. S7C, S8C). Together these results show that hypertonic stress promotes glutamine incorporation into the TCA cycle both *in vitro* and *in vivo*.

NADK2 is required to promote lipid synthesis in response to hypertonic stress

Glutamine oxidation in the TCA cycle produces three molecules of NADH and one FADH2. If the NADH and FADH2 are oxidized in the mitochondrial electron transport chain (mt ETC) oxygen will be consumed. However, we (Fig. 2B) and others found that hypertonicity decreases cellular oxygen consumption rate (*26*). Therefore, the decreased cellular oxygen consumption (Fig. 2B) and simultaneous oxidation of glutamine (Fig. 4) that occur during hypertonic stress could be supported by an alternative pathway to decrease NADH and/or FADH2 accumulation to maintain redox balance in the face of continued oxidative TCA cycling.

One possibility for "re-routing" NADH away from the mt ETC is to convert NADH to NADPH. The nicotinamide nucleotide transhydrogenase (NNT) is an enzyme in the inner mitochondrial membrane that utilizes the H^+ gradient maintained by the mt ETC to transfer electrons from NADH to $NADP^+$, generating NADPH (*34*). However, increased activity of NNT requires increased oxygen consumption which does not happen during hypertonic stress (Fig. 2B and (*35*)). Moreover, the CD cells and the wild-type mice in our experiments are on the C57BL/6J background which lack functional NNT (*36*). An alternate way to re-route TCA-derived NADH away from the mt ETC is through phosphorylation to NADPH. Mitochondrial NAD kinase (NADK2) is a mitochondrial isoform of NADK that plays a critical role in the generation of NADPH (*37*). NADK2 preferentially phosphorylates NAD+, but can also phosphorylate NADH (Fig. 5A) (*38*). Thus, we hypothesized that an increase in NADK2 function could provide an alternate pathway through which mitochondrial NADH could bypass the mt ETC favoring simultaneous oxidative cycling of the TCA and decreased oxygen consumption. Indeed, we found that NaCl increased NADK2 mRNA expression by 2.56-fold ($p=6.31 \times 10^{-136}$ DESeq2) (fig. S9A). We found that hypertonic stress increased NADK2 expression in CD cells (Fig. 5B) and water restriction increased kidney NADK2 expression in wild-type mice (fig. S9B).

Functionally, NADK2 is required to produce mitochondrial NAPDH and mitochondrial NAPDH is necessary for proline synthesis (*37*). Proline increases in both plants and *C. elegans* in response to hypertonic stress *(10, 39-41)*. Proline concentrations also increased significantly in cells treated with NaCl (Fig. 5C), consistent with increased NADK2 activity. To further test if the increase in NADK2 expression was related to hypertonicity-induced transcription factor NFAT5 activation, we performed Cleavage Under targets & Tagmentation (CUT&TAG) and measured NFAT5 occupancy of *Nadk2* regulatory regions before and after hypertonic stress. Increased *Nadk2* promoter occupancy by NFAT5 is associated with active histone mark H3K27 acetylation, indicating that increased NFAT5 occupancy is associated with a functional activating change in the epigenetic landscape at the *Nadk2* promoter (Fig. 5D). Moreover, *Nfat5* knockdown led to a significant decrease in NADK2 expression (Fig. 5E). Together these results indicate that NFAT5 directly regulates NADK2 expression.

To test if NADK2 was required to promote lipid synthesis and accumulation in response to hypertonic stress, we knocked down *Nadk2* in cells and found increased pACC-S79/221 inhibitory phosphorylation (Fig. 5F), and decreased lipid accumulation (Fig. 5G, fig. S10). To confirm the role of NADK2 in the response to hypertonic stress in vivo, we exposed *D. melanogaster* mutants in which

Nadk2 was knocked down (*42*) in the renal epithelium (Malpighian tubule) to hypertonic stress. We found that mutants had significantly higher mortality in response to NaCl hypertonic stress, but not in response to wet starvation (Fig. 5H, fig. S11). While NADK2 is the mitochondrial NAD kinase isoform, *Nadk1a* and *Nadk1b* encode cytoplasmic isoforms(*42*). *Nadk1* and *Nadk1b* knockdown had no effect on survival of *Drosophila* exposed to hypertonic stress (fig. S11C, D). To further examine if NADK2 expression was responsible for the decreased oxygen consumption seen in hypertonic stress, we transfected *Nadk2* mRNA in CD cells and found that NADK2 overexpression significantly decreased OCR and ECAR, recapitulating the effects of high salt (Fig. 5I, J, Fig. 2B). Together, these data confirm the critical role of NADK2 in mitochondrial rewiring in response to hypertonic stress

Hypertonic stress is known to cause increased lipid and proline accumulation in plants (*10, 40*). However, whether NAD kinases play a role in this mechanism is unclear. To test if our observations regarding NADK2 extend to plants, we examined publicly available data sets of *Arabidopsis thaliana* and *Oryza sativa* subjected to various forms of hypertonic stress, and found significant increases in plant isoforms of NADK1, NADK2, and NADK3 (table S1), supporting the notion that in plants NAD kinases are regulated by hypertonicity.

Together, these results show that dehydration stress leads to lipid synthesis and accumulation across biological models, highlighting an evolutionarily conserved mechanism to increase potential water storage.

Discussion

The ability to efficiently generate water from lipids during periods of dehydration provides a survival advantage. Desert animals, plants, and marine mammals have developed the ability to maximize the generation of water from lipids. However, despite association data between hypertonic stress and lipid metabolism (*3, 8, 14, 26, 43-46*), whether and how dehydration prompts lipid accumulation was unknown. In this study we now show that dehydration directly promotes lipid synthesis via mitochondrial remodeling.

We now provide a unifying explanation linking decreases in OCR, changes to mitochondrial metabolism, and lipid accumulation. Our data show that the dynamic metabolic profile of cells under hypertonic stress involves a coordinated response that is regulated by transcription factor NFAT5, which exerts pro-lipogenic effects. These mechanisms explain how to hypertonic stress are related to each other. Our data is consistent with prior studies had observed decreased cellular OCR and pyruvate dehydrogenase inhibition after exposure to hypertonic stress (*26, 46, 47*), as well as others which had shown the accumulation of lipids in animals and plants exposed to hypertonic stress (*6, 7, 48, 49*).

Prior work had shown that the partial absence of NFAT5 promoted increased oxygen consumption and prevented lipid accumulation in mice fed a high fat diet (*27*). We now build on these observations and demonstrate a role for NFAT5 as a critical regulator of fat metabolism in response to hypertonic stress. Whether there is an additive effect in which high-fat feeding and hypertonic stress can synergistically increase NFAT5-mediated obesity is currently unknown.

We found that glutamine incorporation into the TCA was required to synthesize lipids in response to hypertonic stress. Our results also suggest that the simultaneous oxidation of glutamine and decrease in OCR were facilitated by the presence of NADK2, which can divert NADH from the mt ETC via phosphorylation of NADH to NADPH (*38*). This adds to the increasing awareness of NADK2

as a major regulator of mitochondrial metabolism in response to stress; Zhu *et al.* previously reported that NADK2 was critical for the generation of mitochondrial NADPH and proline biosynthesis (*37*) and increased proline biosynthesis is critical in the response to hypertonic stress in plants and *C. elegans* (*39, 41, 50*). Recently Kim *et al.* found that NADK2 fuels mitochondrial fatty acid synthesis and NADK2 depletion decreases the abundance of TCA cycle intermediates, including citrate (*51*). We now identify NADK2 as a key player in the coordination of a metabolic response to hypertonic stress.

Prior work showed that when dehydrated, desert mice (*Notomys alexis*), which are adapted to water stress, shift to beta-oxidative metabolism, while BALB/c laboratory mice synthesize and accumulate fat (*49*). Moreover, Allen et al. have showed that chronic dehydration remodels metabolism and increases metabolic water production (*52*). Recent observations that futile lipid cycling (which produces metabolic water) functions as a metabolic regulator supports the notion that dehydration stress could be involved (*53*). Thus, the impact of the duration of the dehydration stress on lipid synthesis and the timing of lipid synthesis and breakdown remains unclear. Our data now provide a direct link between salt-induced hypertonic stress and lipid accumulation via mitochondrial remodeling.

References

1. R. M. Ortiz, Osmoregulation in marine mammals. *J Exp Biol* **204**, 1831-1844 (2001).
2. J. Rutkowska, E. T. Sadowska, M. Cichon, U. Bauchinger, Increased fat catabolism sustains water balance during fasting in zebra finches. *J Exp Biol* **219**, 2623-2628 (2016).
3. M. A. Ali *et al.*, Effects of long-term dehydration on stress markers, blood parameters, and tissue morphology in the dromedary camel (Camelus dromedarius). *Front Vet Sci* **10**, 1236425 (2023).
4. E. B. Edney, in *Water Balance in Land Arthropods*. (Springer Berlin Heidelberg, Berlin, Heidelberg, 1977), pp. 189-195.
5. W. M. Henne, M. L. Reese, J. M. Goodman, The assembly of lipid droplets and their roles in challenged cells. *EMBO J* **37**, (2018).
6. H. Zhou *et al.*, Insights into plant salt stress signaling and tolerance. *J Genet Genomics* **51**, 16-34 (2024).
7. D. K. Kosma *et al.*, The impact of water deficiency on leaf cuticle lipids of Arabidopsis. *Plant Physiol* **151**, 1918-1929 (2009).
8. M. B. Burg, J. D. Ferraris, N. I. Dmitrieva, Cellular response to hyperosmotic stresses. *Physiol Rev* **87**, 1441-1474 (2007).
9. M. B. Burg, J. D. Ferraris, Intracellular organic osmolytes: function and regulation. *J Biol Chem* **283**, 7309-7313 (2008).
10. C.-J. H. Yun, Kum-Ok. Han, Song-Su. Ri, Hyong-Guan., The effect of salinity stress on the biofuel production potential of freshwater microalgae Chlorella vulgaris YH703. *Biomass and Bioenergy* **127**, (2019).
11. C. Pical, T. Westergren, S. K. Dove, C. Larsson, M. Sommarin, Salinity and hyperosmotic stress induce rapid increases in phosphatidylinositol 4,5-bisphosphate, diacylglycerol pyrophosphate, and phosphatidylcholine in Arabidopsis thaliana cells. *J Biol Chem* **274**, 38232-38240 (1999).
12. J. Fan, L. Zheng, Acclimation to NaCl and light stress of heterotrophic Chlamydomonas reinhardtii for lipid accumulation. *J Biosci Bioeng* **124**, 302-308 (2017).
13. M. Boudsocq, C. Lauriere, Osmotic signaling in plants: multiple pathways mediated by emerging kinase families. *Plant Physiol* **138**, 1185-1194 (2005).
14. A. Gigon, A. R. Matos, D. Laffray, Y. Zuily-Fodil, A. T. Pham-Thi, Effect of drought stress on lipid metabolism in the leaves of Arabidopsis thaliana (ecotype Columbia). *Ann Bot* **94**, 345-351 (2004).
15. A. Mohseni, L. Fan, F. A. Roddick, Impact of microalgae species and solution salinity on algal treatment of wastewater reverse osmosis concentrate. *Chemosphere* **285**, 131487 (2021).
16. L. Abu-Elheiga, M. M. Matzuk, K. A. Abo-Hashema, S. J. Wakil, Continuous fatty acid oxidation and reduced fat storage in mice lacking acetyl-CoA carboxylase 2. *Science* **291**, 2613-2616 (2001).
17. M. Lee *et al.*, Phosphorylation of Acetyl-CoA Carboxylase by AMPK Reduces Renal Fibrosis and Is Essential for the Anti-Fibrotic Effect of Metformin. *J Am Soc Nephrol* **29**, 2326-2336 (2018).
18. Y. Zhao, C. R. Yang, V. Raghuram, J. Parulekar, M. A. Knepper, BIG: a large-scale data integration tool for renal physiology. *Am J Physiol Renal Physiol* **311**, F787-F792 (2016).
19. Y. Kirita, H. Wu, K. Uchimura, P. C. Wilson, B. D. Humphreys, Cell profiling of mouse acute kidney injury reveals conserved cellular responses to injury. *Proc Natl Acad Sci U S A* **117**, 15874-15883 (2020).
20. E. T. B. Olesen, R. A. Fenton, Aquaporin 2 regulation: implications for water balance and polycystic kidney diseases. *Nat Rev Nephrol*, (2021).
21. N. Senoo *et al.*, Cardiolipin, conformation, and respiratory complex-dependent oligomerization of the major mitochondrial ADP/ATP carrier in yeast. *Sci Adv* **6**, eabb0780 (2020).
22. A. Prola *et al.*, Cardiolipin content controls mitochondrial coupling and energetic efficiency in muscle. *Sci Adv* **7**, (2021).
23. D. Tondera *et al.*, SLP-2 is required for stress-induced mitochondrial hyperfusion. *EMBO J* **28**, 1589-1600 (2009).
24. S. Herzig, R. J. Shaw, AMPK: guardian of metabolism and mitochondrial homeostasis. *Nat Rev Mol Cell Biol* **19**, 121-135 (2018).
25. L. C. Gomes, L. Scorrano, Mitochondrial elongation during autophagy: a stereotypical response to survive in difficult times. *Autophagy* **7**, 1251-1253 (2011).
26. T. Ikizawa *et al.*, Mitochondria directly sense osmotic stress to trigger rapid metabolic remodeling via regulation of pyruvate dehydrogenase phosphorylation. *J Biol Chem* **299**, 102837 (2023).
27. H. H. Lee *et al.*, TonEBP/NFAT5 promotes obesity and insulin resistance by epigenetic suppression of white adipose tissue beiging. *Nat Commun* **10**, 3536 (2019).
28. C. Lopez-Rodriguez *et al.*, Loss of NFAT5 results in renal atrophy and lack of tonicity-responsive gene expression. *Proc Natl Acad Sci U S A* **101**, 2392-2397 (2004).
29. W. C. Skarnes *et al.*, A conditional knockout resource for the genome-wide study of mouse gene function. *Nature* **474**, 337-342 (2011).
30. M. A. Lanaspa *et al.*, The expression of aquaporin-1 in the medulla of the kidney is dependent on the transcription factor associated with hypertonicity, TonEBP. *J Biol Chem* **285**, 31694-31703 (2010).

31. C. M. Metallo *et al.*, Reductive glutamine metabolism by IDH1 mediates lipogenesis under hypoxia. *Nature* **481**, 380-384 (2011).
32. A. R. Mullen *et al.*, Reductive carboxylation supports growth in tumour cells with defective mitochondria. *Nature* **481**, 385-388 (2011).
33. P. Keyser, K. Borge-Renberg, D. Hultmark, The Drosophila NFAT homolog is involved in salt stress tolerance. *Insect Biochem Mol Biol* **37**, 356-362 (2007).
34. J. H. Leung *et al.*, Structural biology. Division of labor in transhydrogenase by alternating proton translocation and hydride transfer. *Science* **347**, 178-181 (2015).
35. C. D. Smith, C. A. Schmidt, C. T. Lin, K. H. Fisher-Wellman, P. D. Neufer, Flux through mitochondrial redox circuits linked to nicotinamide nucleotide transhydrogenase generates counterbalance changes in energy expenditure. *J Biol Chem* **295**, 16207-16216 (2020).
36. H. C. Freeman, A. Hugill, N. T. Dear, F. M. Ashcroft, R. D. Cox, Deletion of nicotinamide nucleotide transhydrogenase: a new quantitive trait locus accounting for glucose intolerance in C57BL/6J mice. *Diabetes* **55**, 2153-2156 (2006).
37. J. Zhu *et al.*, Mitochondrial NADP(H) generation is essential for proline biosynthesis. *Science* **372**, 968-972 (2021).
38. J. Du, M. Estrella, K. Solorio-Kirpichyan, P. D. Jeffrey, A. Korennykh, Structure of human NADK2 reveals atypical assembly and regulation of NAD kinases from animal mitochondria. *Proc Natl Acad Sci U S A* **119**, e2200923119 (2022).
39. A. Thiemicke, G. Neuert, Kinetics of osmotic stress regulate a cell fate switch of cell survival. *Sci Adv* **7**, (2021).
40. X. Liang, L. Zhang, S. K. Natarajan, D. F. Becker, Proline mechanisms of stress survival. *Antioxid Redox Signal* **19**, 998-1011 (2013).
41. P. Carillo *et al.*, Nitrogen metabolism in durum wheat under salinity: accumulation of proline and glycine betaine. *Funct Plant Biol* **35**, 412-426 (2008).
42. M. Xu *et al.*, NAD kinase sustains lipogenesis and mitochondrial metabolismthrough fatty acid synthesis. *Cell Rep* **37**, 110157 (2021).
43. M. A. Lanaspa *et al.*, High salt intake causes leptin resistance and obesity in mice by stimulating endogenous fructose production and metabolism. *Proc Natl Acad Sci U S A* **115**, 3138-3143 (2018).
44. Y. Ma, F. J. He, G. A. MacGregor, High salt intake: independent risk factor for obesity? *Hypertension* **66**, 843-849 (2015).
45. N. I. Dmitrieva, M. Boehm, P. H. Yancey, S. Enhorning, Long-term health outcomes associated with hydration status. *Nat Rev Nephrol*, (2024).
46. S. J. Dumas *et al.*, Single-Cell RNA Sequencing Reveals Renal Endothelium Heterogeneity and Metabolic Adaptation to Water Deprivation. *J Am Soc Nephrol* **31**, 118-138 (2020).
47. M. Hamraz *et al.*, Hypertonic external medium represses cellular respiration and promotes Warburg/Crabtree effect. *FASEB J* **34**, 222-236 (2020).
48. F. Alvira-Iraizoz *et al.*, Multiomic analysis of the Arabian camel (Camelus dromedarius) kidney reveals a role for cholesterol in water conservation. *Commun Biol* **4**, 779 (2021).
49. Y. Takei, R. C. Bartolo, H. Fujihara, Y. Ueta, J. A. Donald, Water deprivation induces appetite and alters metabolic strategy in Notomys alexis: unique mechanisms for water production in the desert. *Proc Biol Sci* **279**, 2599-2608 (2012).
50. A. Maggio *et al.*, Does proline accumulation play an active role in stress-induced growth reduction? *Plant J* **31**, 699-712 (2002).
51. D. Kim *et al.*, Mitochondrial NADPH fuels mitochondrial fatty acid synthesis and lipoylation to power oxidative metabolism. *Nat Cell Biol* **27**, 790-800 (2025).
52. M. D. Allen, D. A. Springer, M. B. Burg, M. Boehm, N. I. Dmitrieva, Suboptimal hydration remodels metabolism, promotes degenerative diseases, and shortens life. *JCI Insight* **4**, (2019).
53. A. K. Sharma, R. Khandelwal, C. Wolfrum, Futile lipid cycling: from biochemistry to physiology. *Nat Metab* **6**, 808-824 (2024).

Acknowledgements:
We thank T. Blackwell, A. Morrison, and J. Gavin for the critical reading of the manuscript.
Drosophila stocks obtained from the Bloomington *Drosophila* Stock Center (NIH P40OD018537) were used in this study. Additional stocks were obtained from the Vienna *Drosophila* Resource Center, part of the Vienna Biocenter Core Facilities, a non-profit research infrastructure publicly funded by the Austrian Federal Ministry of Education, Science and Research, and the City of Vienna via the Vienna Business Agency. We are grateful to Drs. Carl Thummel, Julian Dow, Shireen Davies, and Adrian Rothenfluh for sharing *Drosophila* fly lines used in this study.

Funding:

National Institutes of Health grant K08-DK135931 (to JPA)
National Institutes of Health grant R01-DK110358, R01-DK098145 (to ARR)
National Institutes of Health grant AR01DK105550 (to JFR),
National Institutes of Health grant DP5-OD033412 (to AST),
National Institutes of Health grant K08-DK134879 (to FB),
National Institutes of Health grant R38-HL167237 (to JSC),
National Institutes of Health grant DK51265, DK95785, DK62794, (to RCH and MZ),
National Institutes of Health grant DK069921 and DK127589 (to RZ);],
Veterans Affairs Merit Award 00507969 (to RCH),
Veterans Affairs Merit Award I01-BX002196 (to RZ),
National Institutes of Health grant R01-DK081646 (to VHH),
Intramural Research Program of the NIH, NIEHS ES103361-01 (to JAW),
National Institutes of Health grant R21-DK137147 (to JDY),
National Institutes of Health grant R35GM146951 (to JPVM),
National Institutes of Health grant T32CA009582 (to EQJ),
National Institutes of Health grant DK135073, DK020593 (to LL),
National Institutes of Health grant 5K08DK133496 (to IC),
Veterans Affairs Merit Award EB033676, BX004258 (to MHW).

Winkler Family Foundation (JPVM)
Destination Biochemistry Postdoctoral Scholars Program (EQJ)
Department of Defense National Defense Science and Engineering Graduate Fellowship Program (ERP)
Breakthrough T1D Advanced Postdoctoral Fellowship (KV)
Canadian Institutes of Health Research PJT 180476 (PK)
Agriculture and Food Research Initiative Foundational Knowledge of Plant Products (A1103) program, U.S. Department of Agriculture's National Institute of Food and Agriculture, project award no. 2024-67014-42517 and 2021-67013-34009 (D.K.K.)
Fellowship grant from the Uehara Memorial Foundation (RB)
Sharon Anderson fellowship award from the American Society of Nephrology (RB)
Robert Wood Johnson Foundation Harold Amos Medical Faculty Development Program (JPA)
Research Scholar Award from the Southern Society for Clinical Investigation (FB)
The Digital Histology Shared Resource core at Vanderbilt University Medical Center (https://www.vumc.org/dhsr), the Translational Pathology Shared Resource core (P30-CA68485), and the Shared Instrumentation grant S10-OD023475. This work is supported by Metabolomics Workbench/National Metabolomics Data Repository (NMDR) (grant# U2C-DK119886), Common Fund Data Ecosystem (CFDE) (grant# 3OT2OD030544) and Metabolomics Consortium Coordinating Center (M3C) (grant# 1U2C-DK119889). This work was supported in part using the resources of the Center for Innovative Technology (CIT) at Vanderbilt University.

Author contributions:
Conceptualization: JPA, ARR, JCR, FB, AST, JAW, JSC
Investigation: JSC, JPA, ARR, JS, YZ, HJN, CP, GN, EQJ, KV, ETA, JTT, WSY, PK, MM, OV, ERP, JPVM, RB, VHH, SC, KLL, SGC, JBT, CMH, LL, DKK, MW, DS, DAD, CMH, LL, MHW
Methodology: JSC, JPA, ARR, EQJ, JTT, JPC, MAC, JAW
Formal Analysis: JPA, JSC, ARR, FB, EQJ, KV, WSY, ASM, JPC, MAC, KLL, ACS, JAW, YZ, PK, IC, DKK
Resources: JPA, ARR, MHW, RCH, MZ, SDS, JAM, PK, JAW
Project administration: JPA, ARR, JCR, SDS
Visualization: JPA, ARR, FB, ASM, KLL, SGC, HJN, CP, WSY, PK, DKK
Writing – original draft: JPA
Writing – review and editing: JPA, ARR, JCR, JPC, EQJ, KV, ASM, JDY, KLL, SGC, ACS, SDS, JAM, RZ, RCH, JAW, AST, FB, IC
Competing interests: Authors have no competing interests.
Data and materials availability: The untargeted lipidomics data is available at the NIH Common Fund's National Metabolomics Data Repository (NMDR) website, the Metabolomics Workbench, https://www.metabolomicsworkbench.org, where it has been assigned Project ID PR002443. The data can be accessed directly via its Project DOI: http://dx.doi.org/10.21228/M8VG1V.

RNA sequencing data is available at GSE274371.

CUT and Tag data is available at GSE302740. All other data are available in the manuscript or the supplementary materials.

Figure 1

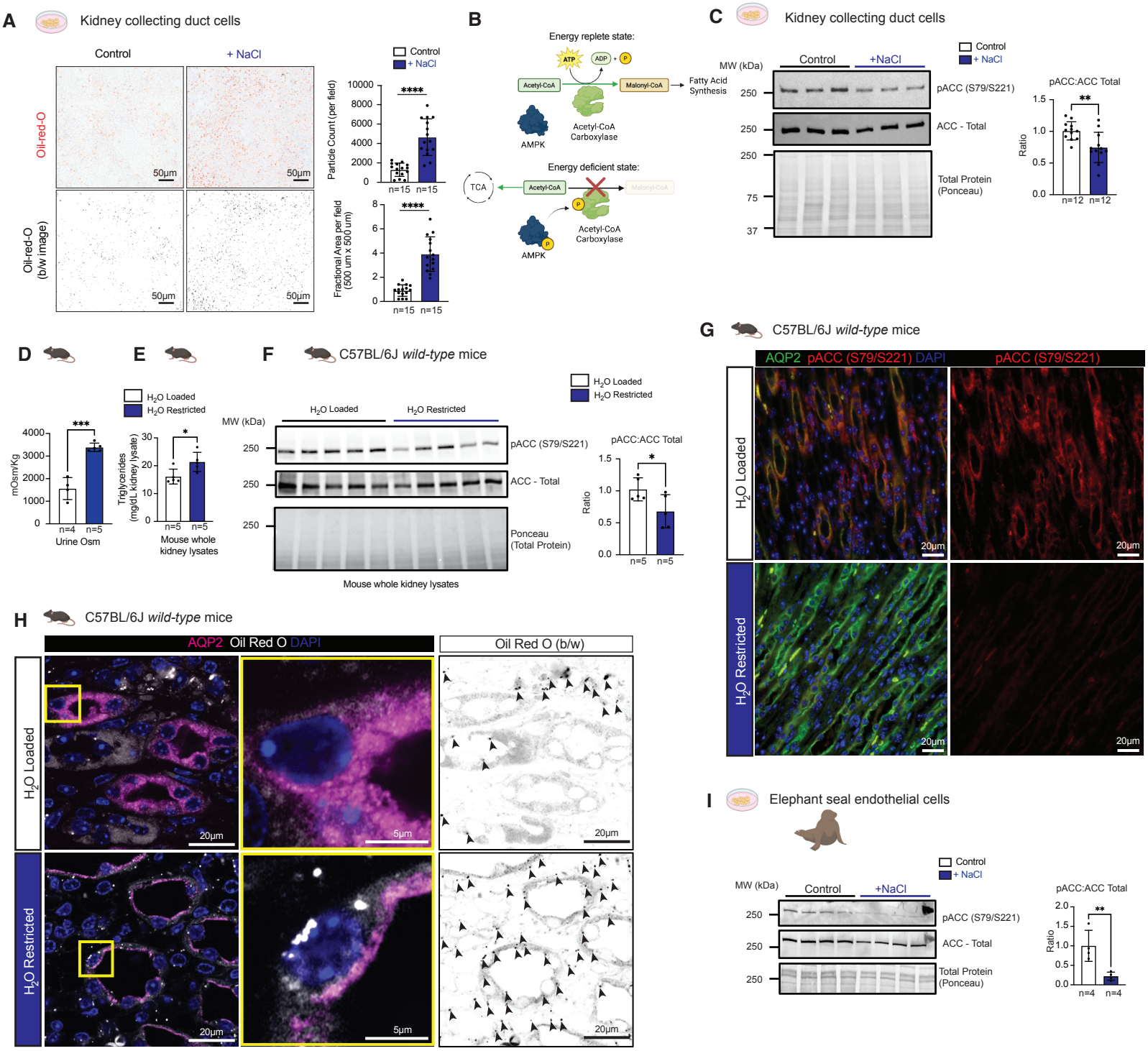
A
Kidney collecting duct cells
Control
+ NaCl
Oil-red-O
Oil-red-O (b/w image)
50µm
Control
+ NaCl
Particle Count (per field)
Fractional Area per field (500 um x 500 um)
****
n=15 n=15
B
Energy replete state:
ATP
ADP
P
Acetyl-CoA
Malonyl-CoA
Fatty Acid Synthesis
Acetyl-CoA Carboxylase
AMPK
Energy deficient state:
TCA
Acetyl-CoA
Malonyl-CoA
Acetyl-CoA Carboxylase
AMPK
C
Kidney collecting duct cells
MW (kDa)
Control
+NaCl
pACC (S79/S221)
ACC - Total
Total Protein (Ponceau)
250
75
37
pACC:ACC Total
Ratio
**
n=12 n=12
D
E
F
C57BL/6J wild-type mice
H2O Loaded
H2O Restricted
mOsm/Kg
***
n=4 n=5
Urine Osm
Triglycerides (mg/dL kidney lysate)
*
n=5 n=5
Mouse whole kidney lysates
MW (kDa)
pACC (S79/S221)
ACC - Total
Ponceau (Total Protein)
pACC:ACC Total
Ratio
Mouse whole kidney lysates
G
C57BL/6J wild-type mice
AQP2 pACC (S79/S221) DAPI
pACC (S79/S221)
H2O Loaded
H2O Restricted
20µm
H
C57BL/6J wild-type mice
AQP2 Oil Red O DAPI
Oil Red O (b/w)
H2O Loaded
H2O Restricted
20µm
5µm
I
Elephant seal endothelial cells
MW (kDa)
Control
+NaCl
pACC (S79/S221)
ACC - Total
Total Protein (Ponceau)
pACC:ACC Total
Ratio
**
n=4 n=4

Fig. 1. NaCl hypertonic stress induces lipid accumulation in cells. (**A**) Oil-red-o lipid droplet staining in CD cells treated with 100 mmol NaCl vs control 12 hours. (B) Acetyl-CoA Carboxylase is the rate limiting step in fatty acid synthesis and can be inhibited by AMP activated protein kinase (AMPK) via phosphorylation in states of energy depletion. (C) Immunoblots of total Acetyl-CoA Carboxylase (ACC) and pACC-S79/221 from kidney collecting duct cell lysates treated with 100 mmol NaCl vs control. (D) Urine osmolality (mOsm/Kg) and whole-kidney lysate triglyceride content from wild-type C57BL/6J mice after 24h water loading or water restriction. (F) Immunoblots of total ACC and pACC-S79/221 from whole kidney lysates of mice after water loading or water restriction. (G) Immunofluorescence of pACC-S79/221 and water channel Aquaporin 2 (AQP2), a collecting duct marker, in kidneys from water-loaded or water-restricted mice. (H) Oil-red-O lipid droplet and AQP2 immunofluorescent staining in kidneys from water-loaded and water-restricted mice. (I) Immunoblot of total Acetyl-CoA Carboxylase (ACC) and pACC-S79/221 from elephant seal primary endothelial cell lysates treated with 100 mmol NaCl vs control. Data presented as mean +/- SD. Data in A,C,D,E,F, and I analyzed with a two-tailed Student's t-test. * $p<0.05$, ** $p<0.01$, *** $p<0.001$, ****$p<0.0001$, n as indicated in each panel. CD – Kidney collecting duct cells

Figure 2

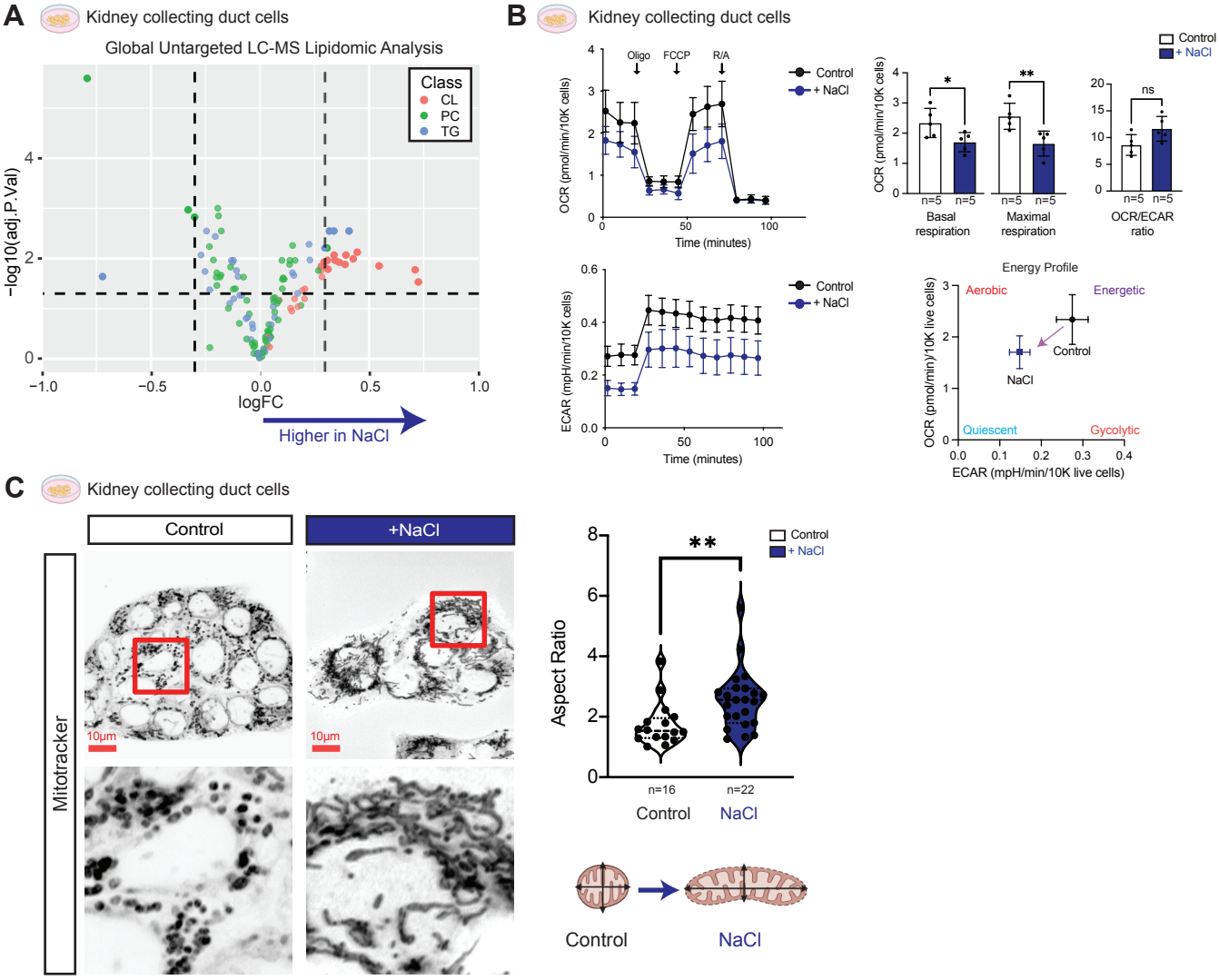
A
Kidney collecting duct cells
Global Untargeted LC-MS Lipidomic Analysis
Class
CL
PC
TG
−log10(adj.P.Val)
logFC
Higher in NaCl
B
Kidney collecting duct cells
Oligo
FCCP
R/A
Control
+ NaCl
OCR (pmol/min/10K cells)
Time (minutes)
Basal respiration
Maximal respiration
OCR/ECAR ratio
ns
ECAR (mpH/min/10K cells)
Energy Profile
Aerobic
Energetic
Quiescent
Gycolytic
OCR (pmol/min)/10K live cells)
ECAR (mpH/min/10K live cells)
C
Kidney collecting duct cells
Control
+NaCl
Mitotracker
10µm
Aspect Ratio
n=16
n=22
Control
NaCl

Fig. 2. NaCl hypertonic stress alters mitochondrial metabolism. (A) Global untargeted LC-MS/MS lipidomic analysis of lipids by class in NaCl-treated CD cells vs controls. (B) Live metabolic cell profiling of NaCl treated CD cells. (C) Immunofluorescence mitochondrial aspect ratio analysis. Data in A LogFC of NaCl vs control cells plotted relative to -log10(adj. p value). Data in B presented as mean +/- SD and analyzed with Student's t-test. Data in C presented as mean +/- SD box-violin plot and analyzed with a Mann-Whitney Test *$p<0.05$, ** $p<0.01$, n as indicated in each panel. CL - cardiolipin, TG - triglyceride, PC – Phosphatidylcholine, OCR – oxygen consumption rate, ECAR – extracellular acidification rate, CD – Kidney collecting duct cells.

Figure 3

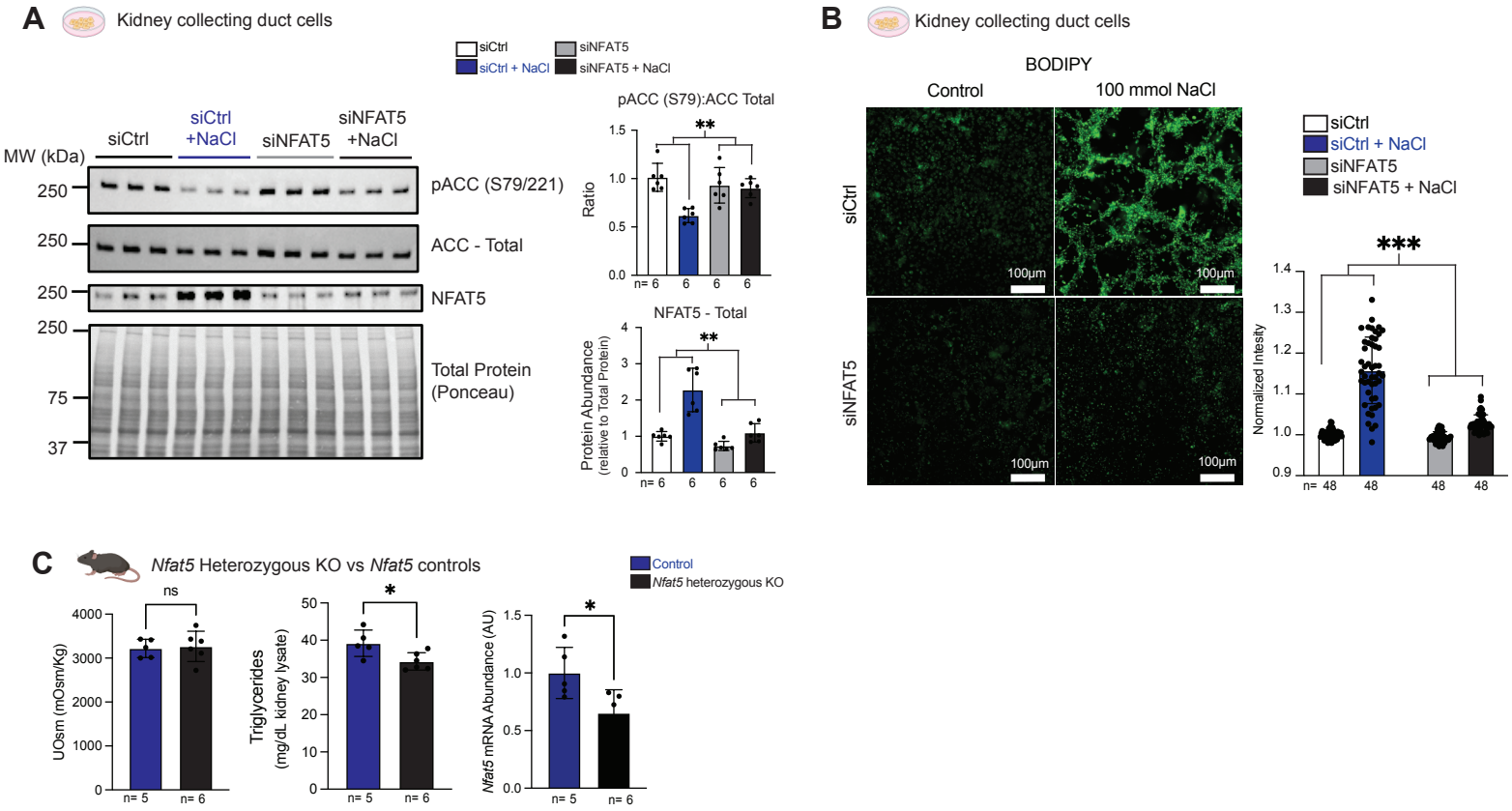
A
Kidney collecting duct cells
siCtrl
siCtrl + NaCl
siNFAT5
siNFAT5 + NaCl
MW (kDa)
siCtrl
siCtrl +NaCl
siNFAT5
siNFAT5 +NaCl
250
250
250
250
75
37
pACC (S79/221)
ACC - Total
NFAT5
Total Protein (Ponceau)
pACC (S79):ACC Total
Ratio
NFAT5 - Total
Protein Abundance (relative to Total Protein)
n= 6 6 6 6
B
Kidney collecting duct cells
BODIPY
Control
100 mmol NaCl
siCtrl
siNFAT5
100µm
Normalized Intesity
n= 48 48 48 48
C
Nfat5 Heterozygous KO vs Nfat5 controls
Control
Nfat5 heterozygous KO
ns
UOsm (mOsm/Kg)
Triglycerides (mg/dL kidney lysate)
Nfat5 mRNA Abundance (AU)
n= 5 n= 6

Fig. 3. NFAT5 is required for hypertonicity induced lipid synthesis. (**A**) Immunoblots of total Acetyl-CoA Carboxylase (ACC), pACC-S79/221, and NFAT5 in CD cells transfected with si*Nfat5* vs siCtrl treated with NaCl or control. (B) Immunofluorescence of BODIPY-stained lipid droplets in CD cells treated with siCtrl or si*Nfat5* +/- NaCl. (C) Urine osmolality, kidney lysate triglycerides, and *Nfat5* mRNA in NFAT5 heterozygous KO mice vs controls after water restriction. Data in A and B presented as mean +/- SD, analyzed with two-way ANOVA with NaCl and siRNA as the independent variables. **$p<0.01$ for the interaction, n as noted in figure. Data in C presented as mean +/- SD analyzed with a two-tailed Student's t-test *$p<0.05$. n as indicated in each panel. CD – Kidney collecting duct cells

Figure 4

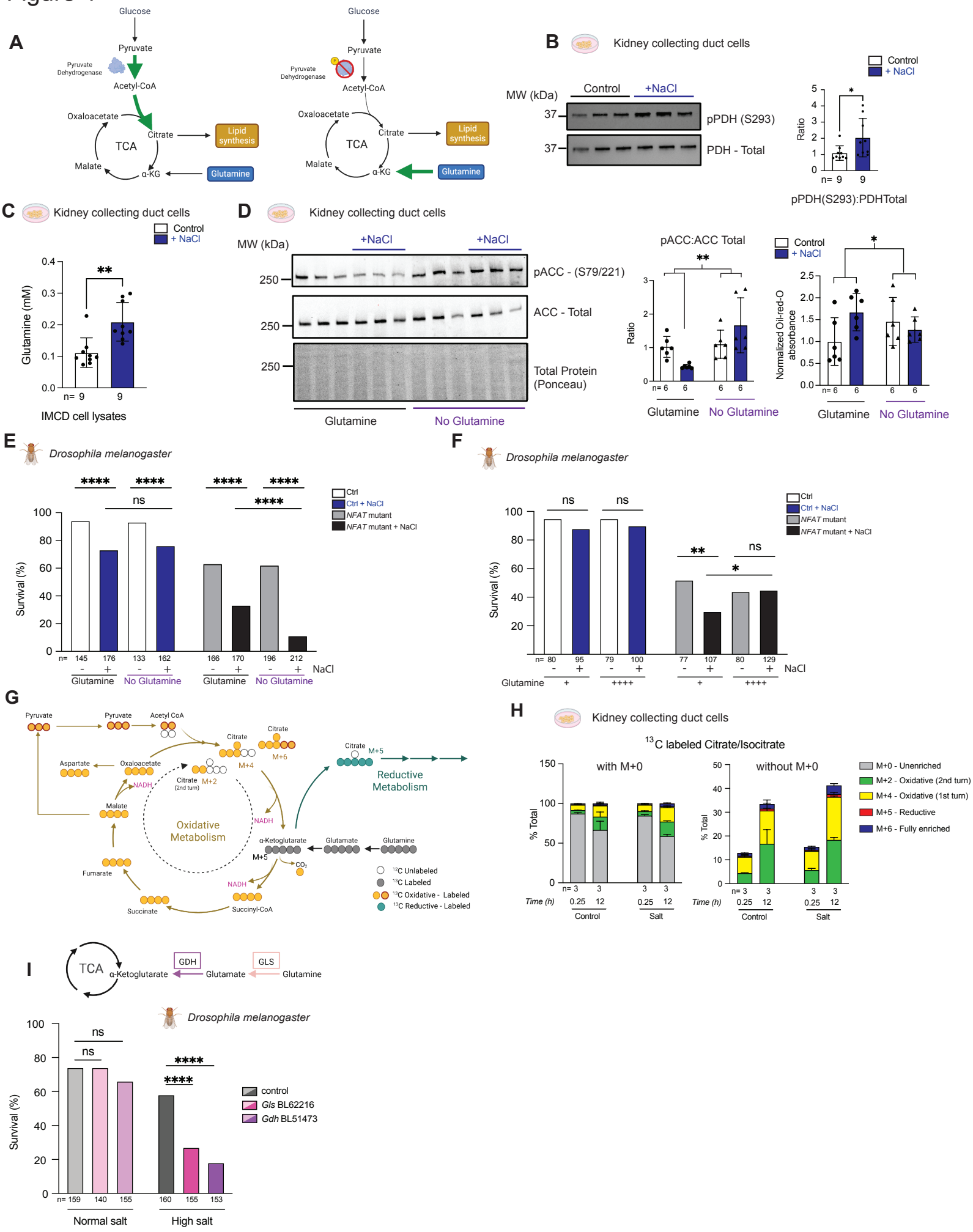
A
Glucose
Pyruvate
Pyruvate Dehydrogenase
Acetyl-CoA
Oxaloacetate
Citrate
TCA
Malate
α-KG
Lipid synthesis
Glutamine
B
Kidney collecting duct cells
Control
+ NaCl
MW (kDa)
37
pPDH (S293)
PDH - Total
Ratio
n= 9 9
pPDH(S293):PDHTotal
C
Kidney collecting duct cells
Glutamine (mM)
n= 9 9
IMCD cell lysates
D
Kidney collecting duct cells
MW (kDa)
250
pACC - (S79/221)
ACC - Total
Total Protein (Ponceau)
pACC:ACC Total
Normalized Oil-red-O absorbance
Glutamine
No Glutamine
E
Drosophila melanogaster
Survival (%)
Ctrl
Ctrl + NaCl
NFAT mutant
NFAT mutant + NaCl
n= 145 176 133 162 166 170 196 212
NaCl
F
Drosophila melanogaster
n= 80 95 79 100 77 107 80 129
G
Pyruvate
Acetyl CoA
Citrate
Aspartate
Oxaloacetate
Malate
Fumarate
Succinate
Succinyl-CoA
α-Ketoglutarate
Glutamate
Glutamine
Oxidative Metabolism
Reductive Metabolism
NADH
M+2
M+4
M+5
M+6
12C Unlabeled
13C Labeled
13C Oxidative - Labeled
13C Reductive - Labeled
H
Kidney collecting duct cells
13C labeled Citrate/Isocitrate
with M+0
without M+0
% Total
M+0 - Unenriched
M+2 - Oxidative (2nd turn)
M+4 - Oxidative (1st turn)
M+5 - Reductive
M+6 - Fully enriched
Time (h)
Control
Salt
I
TCA
α-Ketoglutarate
GDH
Glutamate
GLS
Glutamine
Drosophila melanogaster
control
Gls BL62216
Gdh BL51473
n= 159 140 155 160 155 153
Normal salt
High salt

Fig. 4. Glutamine is required for hypertonicity-induced lipid synthesis. (A) Pyruvate dehydrogenase (PDH) is inhibited via phosphorylation. (B) Immunoblotting for phosphorylated pPDH (S293) and total PDH in CD cells treated with NaCl vs control. (C) Intracellular glutamine levels in CD cells treated with NaCl vs control. (D) Immunoblotting for phosphorylated acetyl-coA carboxylase (pACC-S79/221), total ACC and normalized oil-red-o absorbance in kidney collecting duct cell lysates treated with NaCl vs control in presence or absence of glutamine. (E, F) Survival analysis of control or *NFAT* mutant *D. melanogaster* after indicated feeding paradigms (fig S11). (G) Metabolic pathways of universally labeled C13 glutamine. (H) Distribution of ^{13}C-enriched isotopologues of citrate/isocitrate in IMCDs treated with control or NaCl hypertonic stress. (I) Survival analysis of *D. melanogaster Gls* (BL62216) and *Gdh* (BL51473) renal epithelial knockdown flies when exposed to NaCl hypertonic stress and water restriction. Data in B and C presented as mean +/- SD, analyzed with a two-tailed student's t-test *$p<0.05$, ** $p<0.01$. Data in D presented as mean +/- SD, analyzed with two-way ANOVA with NaCl and glutamine supplementation as the independent variables. *$p<0.05$, **$p<0.01$ for the interaction, n as noted in figure. Data in E,F, and I presented as % survival analyzed with Fischer's exact test *****$p<0.0001$. n as indicated in each panel. CD – Kidney collecting duct cells

Figure 5

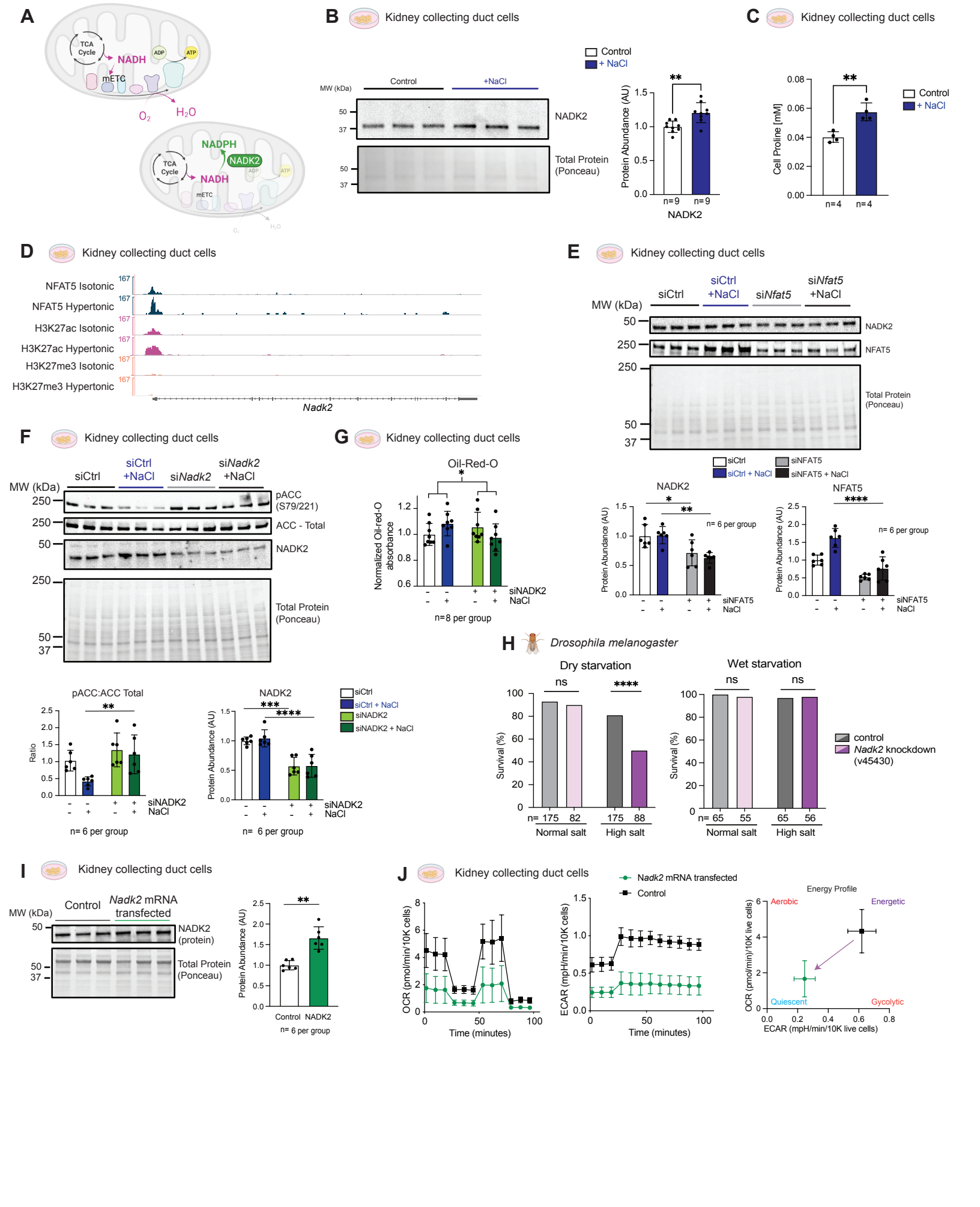
A
TCA Cycle
NADH
ADP
ATP
mETC
O_2
H_2O
NADPH
NADK2
B
Kidney collecting duct cells
Control
+NaCl
MW (kDa)
NADK2
Total Protein (Ponceau)
Protein Abundance (AU)
n=9
n=9
C
Kidney collecting duct cells
Cell Proline [mM]
n=4
n=4
D
Kidney collecting duct cells
NFAT5 Isotonic
NFAT5 Hypertonic
H3K27ac Isotonic
H3K27ac Hypertonic
H3K27me3 Isotonic
H3K27me3 Hypertonic
Nadk2
E
Kidney collecting duct cells
siCtrl
siCtrl +NaCl
siNfat5
siNfat5 +NaCl
NFAT5
siNFAT5
siNFAT5 + NaCl
n= 6 per group
F
Kidney collecting duct cells
siNadk2
siNadk2 +NaCl
pACC (S79/221)
ACC - Total
pACC:ACC Total
Ratio
siNADK2 + NaCl
n= 6 per group
G
Kidney collecting duct cells
Oil-Red-O
Normalized Oil-red-O absorbance
siNADK2
NaCl
n=8 per group
H
Drosophila melanogaster
Dry starvation
Wet starvation
Survival (%)
control
Nadk2 knockdown (v45430)
Normal salt
High salt
I
Kidney collecting duct cells
Nadk2 mRNA transfected
NADK2 (protein)
J
Kidney collecting duct cells
Nadk2 mRNA transfected
Control
OCR (pmol/min/10K cells)
Time (minutes)
ECAR (mpH/min/10K cells)
Energy Profile
Aerobic
Energetic
Quiescent
Gycolytic
OCR (pmol/min)/10K live cells)
ECAR (mpH/min/10K live cells)

Fig. 5. NADK2 is required for hypertonic stress-induced lipid synthesis. (A) Mitochondrial NADK2 can directly phosphorylate NADH generated by the tricarboxylic acid cycle (TCA) and shunt it away from the mitochondrial electron transport chain (mt ETC). (B) Immunoblots of NADK2 in whole cell lysates from CD cells. (C) Cell proline concentration in CD cells treated with NaCl vs controls. (D) Cleavage Under targets & Tagmentation (CUT&TAG) of CD cells under isotonic and hypertonic conditions showing NFAT5 occupancy in the promoter region of *Nadk2*, H3K27ac (positive control), and H3K27me3 (negative control). y-axis denotes reads per genomic content (RPGC). (E) Immunoblots for NADK2 and NFAT5 in cells transfected with siRNA targeting *Nfat5* +/- NaCl. (F) Immunoblots for NADK2, pACC (S279/221) and total ACC in cells transfected with siRNA targeting *Nadk2* +/- NaCl. (G) Normalized oil-red-o absorbance in cells treated with si*Nadk2* +/- NaCl. (H) Survival analysis of *D. melanogaster* renal epithelial *Nadk2* knockdown vs. control when exposed to hypertonic stress. (I) Immunoblots of kidney collecting duct cell lysates transfected with *Nadk2* mRNA. (J) Live metabolic cell profiling of CD cells transfected with *Nadk2*. Data in B,C, and I presented as mean +/- SD. **$p<0.01$ analyzed with two-tailed student's t-test, n as noted. Data in E,F, and G presented as mean +/- SD analyzed with two-way ANOVA with NaCl and respective siRNA as independent variables and Šídák's multiple comparisons test, *$p<0.05$, **$p<0.01$, ***$p<0.001$, ****$p<0.0001$, interaction between variables significant in G *$p<0.05$, not significant in F. Data in H presented as % survival analyzed with Fischer's exact test **$p<0.01$. Data in J presented as mean +/- SD, n=5 biologic replicates per time point. CD – Kidney collecting duct cells